Active hair-bundle movements can amplify a hair cell's response to oscillatory mechanical stimuli

Pascal Martin and A. J. Hudspeth*

Howard Hughes Medical Institute and Laboratory of Sensory Neuroscience, The Rockefeller University, 1230 York Avenue, New York, NY 10021-6399

Contributed by A. J. Hudspeth, October 21, 1999

To enhance their mechanical sensitivity and frequency selectivity, hair cells amplify the mechanical stimuli to which they respond. Although cell-body contractions of outer hair cells are thought to mediate the active process in the mammalian cochlea, vertebrates without outer hair cells display highly sensitive, sharply tuned hearing and spontaneous otoacoustic emissions. In these animals the amplifier must reside elsewhere. We report physiological evidence that amplification can stem from active movement of the hair bundle, the hair cell's mechanosensitive organelle. We performed experiments on hair cells from the sacculus of the bullfrog. Using a two-compartment recording chamber that permits exposure of the hair cell's apical and basolateral surfaces to different solutions, we examined active hair-bundle motion in circumstances similar to those *in vivo*. When the apical surface was bathed in artificial endolymph, many hair bundles exhibited spontaneous oscillations of amplitudes as great as 50 nm and frequencies in the range 5 to 40 Hz. We stimulated hair bundles with a flexible glass probe and recorded their mechanical responses with a photometric system. When the stimulus frequency lay within a band enclosing a hair cell's frequency of spontaneous oscillation, mechanical stimuli as small as ±5 nm entrained the hair-bundle oscillations. For small stimuli, the bundle movement was larger than the stimulus. Because the energy dissipated by viscous drag exceeded the work provided by the stimulus probe, the hair bundles powered their motion and therefore amplified it.

Hair cells of the vertebrate inner ear increase their sensitivity by amplifying mechanical inputs (reviewed in ref. 1). When a sound stimulates the auditory system, components such as the basilar and tectorial membranes, as well as the hair bundles themselves, are set into mechanical oscillation. Because these structures are immersed in a viscous fluid, however, the amplitude of motion is limited by viscous dissipation. The ear's active process has been hypothesized to provide work—in effect "negative damping"—that counters energy losses to viscous drag (2). Amplification is nonlinear and accounts for some of the nonlinearities observed in cochlear performance (reviewed in ref. 3). The strength of amplification rises as the sound level declines; in a quiet environment, the amplifier is so active that it produces spontaneous otoacoustic emissions. Amplification operates over a narrow range of basilar-membrane and hair-bundle deflections. As measured by laser-interferometric velocimetry in the chinchilla, the basilar-membrane excursion varies only between ±3 nm and ±30 nm over a 10,000-fold range of stimulation (reviewed in refs. 4 and 5).

The mechanism of cochlear amplification remains uncertain. In the mammalian cochlea, outer hair cells constitute the principal amplifiers. The active process in these cells is thought to be electromotility, or changes in cellular length in response to variations in transmembrane potential (reviewed in refs. 6 and 7). These movements ensue from voltage-driven rearrangements of intrinsic membrane proteins. There nevertheless remain reasons to doubt that this mechanism can account for the active process (reviewed in ref. 8). In particular, the known properties of electromotility do not suffice to produce amplification (9). Moreover, there have been no observations of spontaneous outer-hair-cell contractions that might underlie spontaneous otoacoustic emissions.

An alternative candidate for the cochlear amplifier is active hair-bundle motion. This mechanism could account for amplification in nonmammalian vertebrates, which lack outer hair cells (reviewed in refs. 1 and 10), and may be relevant in mammalian hair cells as well (11). Hair bundles can respond to force pulses by producing oscillatory movements or abrupt twitches (12–16). In addition, bundles can oscillate spontaneously with amplitudes in excess of those expected for brownian motion (12, 13, 15, 17). Because these active responses have been observed only sporadically, however, the mechanism of active hair-bundle motion remains uncertain. Although the hair bundle's myosin-based adaptation mechanism (reviewed in refs. 18 and 19) may be required for amplification (15), the force-generating element may be the transduction channel itself (14, 15, 20).

Studies of hair-bundle mechanics generally have been performed in an ionic milieu resembling ordinary extracellular fluid, rather than in the low-Na^+, low-Ca^{2+} endolymph that normally bathes hair bundles. Several features of the experimental environment may have diminished the amplificatory capacity of hair cells. First, in the presence of relatively high concentrations of Na^+ and Ca^{2+}, cells may suffer from the metabolic load imposed by the necessity of extruding these cations after their entry through transduction channels. Next, elevated Ca^{2+} flux through these channels may overactivate components of the amplificatory mechanism. Consistent with this possibility, reducing the Ca^{2+} concentration to its physiological level transforms the bundle's twitches into oscillatory responses near the cell's characteristic frequency (15).

A final concern about the conventional recording environment pertains to the possibility that transduction channels mediate amplification. The opening and closing of transduction channels during stimulation reduces hair-bundle stiffness, a phenomenon termed gating compliance (14). Under some circumstances the hair bundle's stiffness might even become negative (5, 21). As with negative resistance in electronics, such a situation would provide a substrate for amplification. Because Ca^{2+} affects hair-bundle stiffness (16), amplification might be enhanced in the presence of a physiological concentration of this ion.

Using a two-compartment recording environment that permits exposure of the hair cell's apical and basolateral surfaces to different solutions, we have examined active hair-bundle movements in circumstances similar to those *in vivo*. By driving bundles with sinusoidal stimuli and measuring their mechanical properties with a flexible stimulus fiber, we have inquired whether hair bundles can do useful work against an external load.

Abbreviation: NMDG, *N*-methyl-D-glucamine.

*To whom reprint requests should be addressed at: The Rockefeller University, Box 314, 1230 York Avenue, New York, NY 10021-6399. E-mail: hudspaj@rockvax.rockefeller.edu.

The publication costs of this article were defrayed in part by page charge payment. This article must therefore be hereby marked "*advertisement*" in accordance with 18 U.S.C. §1734 solely to indicate this fact.

Materials and Methods

Experimental Preparation. The sacculus dissected from the internal ear of an adult bullfrog (*Rana catesbeiana*) was placed in oxygenated standard saline solution containing 110 mM Na^+, 2 mM K^+, 4 mM Ca^{2+}, 118 mM Cl^-, 3 mM D-glucose, and 5 mM Hepes. After otoconia and extramacular tissue had been removed, the otolithic membrane's attachment to hair bundles was loosened by exposing the organ for 30 min at 21°C to 40 mg·1^{-1} of protease (type XXIV, Sigma). The otolithic membrane then was gently removed with forceps.

The saccular macula was sealed over a 1-mm hole in a plastic coverslip with tissue-compatible acrylic adhesive (Iso-Dent, Ellman International, Hewlett, NY) and mounted, with the hair bundles directed upward, as the partition in a thin two-compartment chamber. The lower compartment was filled with oxygenated standard saline solution. Either of two oxygenated solutions was placed in the upper chamber, where it bathed the hair bundles. One medium was artificial endolymph containing 2 mM Na^+, 118 mM K^+, 0.25 mM Ca^{2+}, 118 mM Cl^-, 3 mM D-glucose, and 5 mM Hepes. The alternative solution, *N*-methyl-D-glucamine (NMDG) endolymph, comprised 2 mM Na^+, 3 mM K^+, 0.25 mM Ca^{2+}, 110 mM NMDG, 119 mM Cl^-, 3 mM D-glucose, and 5 mM Hepes. For each of the three saline solutions, the pH was 7.2–7.3 and the osmotic strength approximately 230 mmol·kg^{-1}. Experiments were conducted at a room temperature of 21°C.

Microscopic Apparatus. The experimental chamber was mounted on the rotating stage of an upright microscope (MPS, Zeiss) secured to an antivibration table (63-543, TMC, Peabody, MA). The preparation was viewed through a 40×, Achroplan water-immersion objective lens of numerical aperture 0.75; the image was magnified 1.6× with the microscope's accessory lens system. During the attachment of a stimulus fiber to a hair bundle, the preparation was observed with Nomarski optics and 10× oculars. For experimental measurements, the polarizer was removed from the light path and the image was projected through an 8× ocular situated in the trinocular tube.

A 100-W mercury lamp provided illumination for experiments. To protect the preparation from photodamage, the illumination pathway was equipped with an infrared-reflecting hot mirror (Edmund Industrial Optics, Barrington, NJ) and an interference filter that transmitted ±40 nm about a center wavelength of 500 nm.

Stimulation. Flexible stimulus fibers were pulled from 1.2-mm-diameter borosilicate-glass rods as described (13–15). Each fiber had a length of 150–350 μm and a diameter of 0.3–0.8 μm after sputter-coating with gold-palladium to increase optical contrast. The characteristics of each fiber were determined by measurement of the power spectrum of its brownian motion in water (13). For the reported experiments, fiber stiffnesses lay in the range 100 to 280 μN·m^{-1} and their drag coefficients in the range 60 to 130 nN·s·m^{-1}; the time constants for fiber responsiveness were 131–1,010 μs.

During an experiment, the base of the stimulus fiber was displaced by a high-frequency piezoelectrical stimulator (P-835.10, Physik Instrumente, Waldbronn, Germany), which was positioned with a Huxley micromanipulator. An eight-pole, low-pass Bessel filter with a half-power frequency of 2 kHz conditioned the stimulus-command signals delivered to the stimulator's power supply (P-870, Physik Instrumente).

Photometric Recording. The stimulus fiber's tip was imaged at a magnification of 1,000× on a dual photodiode (UV-140-2, EG&G Electro-Optics, Salem, MA), which yielded an output linearly proportional to the displacement of the stimulus fiber and with a resolution of ~1 nm. The image was centered on the detector by translating the photodiode system with a stepping-motor microdrive and controller (850B-05 and PMC100, Newport, Irvine, CA). To mechanically decouple the photometric apparatus, it was placed on a separate platform mounted above the microscope.

After a suitable hair bundle had been identified, the tip of the horizontally mounted stimulus fiber was brought into contact with the bulbous tip of the kinocilum; freshly prepared fibers adhered tightly. At the outset of each stimulation, the photometric system was calibrated by transiently displacing the detector 20 μm with a piezoelectric micromanipulator and controller (PZL-060-11 and PZ-150 M, Burleigh Instruments, Fishers, NY). This procedure elicited an output equivalent to that of a 20-nm displacement of the stimulus fiber, a signal that could be used as a calibration despite variation in the light transmission and contrast of the specimen. Additional details of the stimulation and recording system have been published (15).

Data Acquisition and Analysis. Stimulation and recording were performed under the control of a computer (P6400 GX1, Dell Computer, Round Rock, TX) running LABVIEW software (version 5.0, National Instruments, Austin, TX). Stimulus commands and experimental control signals were provided by a dedicated interface (AT-AO-10, National Instruments). Before sampling, responses were conditioned with an eight-pole Bessel anti-aliassing filter adjusted to a low-pass half-power frequency of 1 kHz. A multipurpose interface card (PCI-MIO-16E-1, National Instruments) conducted signal acquisition and analog-to-digital conversion with a precision of 12 bits and a sampling rate of 2–5 kHz.

Data were analyzed with MATHEMATICA (version 3.0 PPC, Wolfram Research, Champaign, IL). Records of the positions of the stimulus fiber's base and tip were smoothed by forming the running average of a number of points equal to one-tenth of a cycle. After interpolation had been used to adjust the data so that each cycle comprised an integer number of data points, calculations were performed on the data arrays. The results then were averaged across cycles.

Results

We characterized the mechanical responsiveness of hair bundles in endolymph-like solutions by mounting an epithelial preparation of the frog's sacculus in a two-compartment recording chamber. While the basolateral cellular surfaces were exposed to standard saline solution, the apical surfaces including the hair bundles experienced either artificial endolymph or a similar solution in which most of the K^+ had been replaced by NMDG. This substance carries negligible transduction current, but does not interfere with the permeation of other cations (22). When artificial endolymph was used, an imperfect seal between the two compartments sometimes permitted leakage of this K^+-rich fluid into the basal compartment, depolarizing the hair cells and abbreviating the experiment. NMDG-based endolymph, in contrast, extended the lifetime of the preparation to as many as 3 hr. After ascertaining that responses were similar in both solutions, we routinely used NMDG in subsequent experiments.

A striking characteristic of either recording environment was the widespread occurrence of spontaneously moving hair bundles. In well-dissected preparations, many of the bundles in a microscopic field of view displayed oscillations large and slow enough to be detected by a trained eye. The bundles appeared to move independently; there was no evidence that the frequency or phase of motion was shared by adjacent cells.

Spontaneous hair-bundle motion also was readily apparent in records made by attaching the tip of a flexible stimulus fiber to a bundle and monitoring its displacement with a photometric system (Fig. 1 *A* and *E*). The frequencies of spontaneous

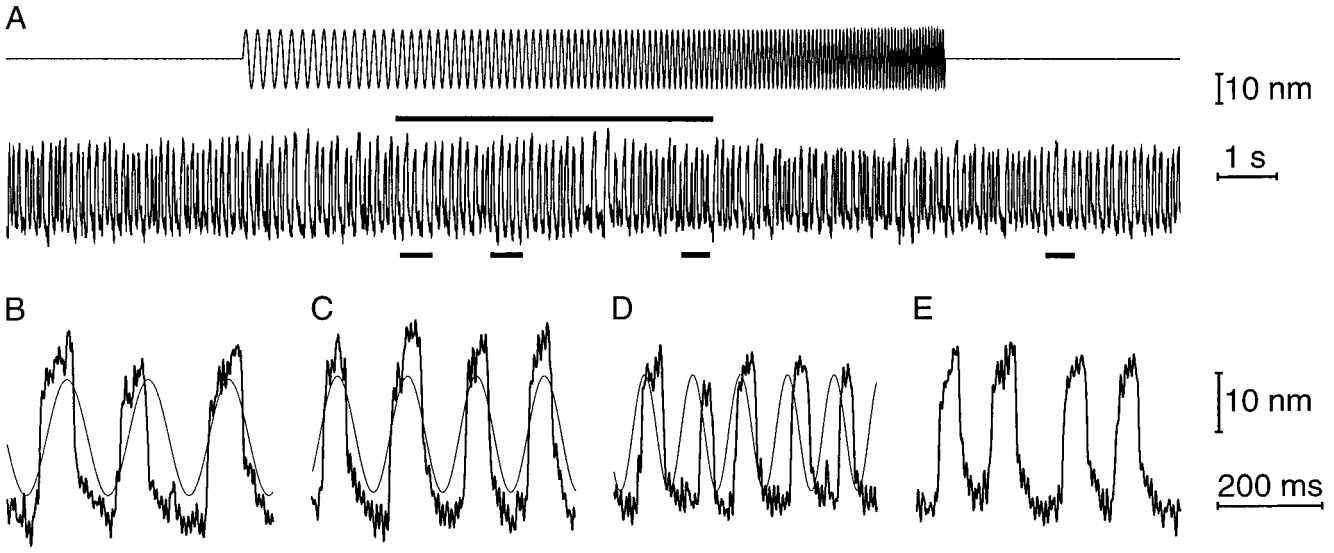

Fig. 1. Entrainment of the hair bundle's spontaneous oscillations by ±10-nm sinusoidal displacement of a stimulus fiber's base. The stimulus frequency was swept from 5 Hz to 21 Hz. (*A*) Shown are the motion of the stimulus fiber's base (*Upper*) and the resultant movement of the fiber's tip and the attached hair bundle (*Lower*). Note that, in the absence of stimulation, the hair bundle oscillated spontaneously at a frequency of ~9 Hz. The horizontal bar above the lower trace delimits the frequency domain of 6–12 Hz in which oscillation was entrained by the stimulus. Note, however, that the bundle transiently escaped entrainment twice during this interval. The four bars below the trace mark the regions shown in the subsequent panels. Baseline drift of as much as 15 nm·s^{-1} was removed from the record. (*B*) At a stimulus frequency of ~6.5 Hz, the movement of the fiber's tip led that of its base. In this and *C* and *D*, the stimulus (thin trace) is superimposed on the response (thick trace). (*C*) For stimulation at ~7.5 Hz, the response and the drive were roughly in phase. (*D*) For a stimulus frequency of ~11 Hz, the fiber's tip motion lagged that of its base. (*E*) The hair bundle's limit-cycle oscillation displayed two components, a rapid stroke in each direction followed by a slower relaxation.

oscillation were 5–40 Hz and the excursions 25–50 nm. The oscillation waveform was not sinusoidal, for the movement in each direction displayed two distinct components (Fig. 1*E*): a rapid stroke lasting ~1 ms was followed by a slow relaxation, with a time constant of ~30 ms, before a stroke in the opposite direction.

Mechanical Response to Oscillatory Stimulation. Hair bundles displayed spontaneous oscillations considerably larger than brownian motion (12, 13): they were mechanically active. By applying sinusoidal stimuli to hair bundles, we assessed the possibility that their movements could be entrained so that the bundles provided useful work against an external load. Entrainment of bundle motion was routine anywhere in the macula when the stimulus fiber's base was displaced with an amplitude larger than ±50 nm. For stimulus amplitudes comparable to or smaller than the spontaneous hair-bundle motion, however, entrainment required that the driving frequency be near the hair cell's frequency of spontaneous oscillation. For the cell in Fig. 1*A*, entrainment with a ±10-nm stimulus occurred within the frequency band of 9 ± 3 Hz. When the stimulus frequency was significantly lower or higher than this characteristic frequency, entrainment failed to occur and spontaneous oscillations persisted. Respecting that constraint, a bundle could be driven with stimuli as small as ±5 nm. Strikingly, even though the stimulus was delivered with a flexible fiber, a hair bundle often oscillated through a distance as great as the motion of the fiber's base. For small stimuli, the bundle's motion could even exceed that of the fiber's base. In these cases, the hair bundle actually pulled the fiber's tip farther in one or both directions than it would have moved if detached from the bundle.

A crucial characteristic of recordings from an active hair bundle was the phase relation between the movements of the tip and base of the stimulus fiber. In a passive system driven at relatively low frequencies, the fiber's tip and the attached hair bundle would be expected to move in phase with the fiber's base or to lag slightly as a result of viscous drag. For active hair bundles, however, the pattern was more complex. When the stimulus frequency exceeded the characteristic frequency, the response displayed a phase lag (Fig. 1*D*). Stimulation at or near the characteristic frequency yielded an in-phase response (Fig. 1*C*). Finally, when the stimulus frequency was lower than a bundle's characteristic frequency, the motion of the fiber's tip led that of its base (Figs. 1*B* and 2 *A* and *B*). Entrainment with such a phase lead could not occur in a passive system.

Quantitative Analysis of Amplification. Because the hair bundle is immersed in a fluid, viscous drag opposes the bundle's motion and continuously withdraws energy. To sustain hair-bundle oscillation, work must be provided to counterbalance viscous dissipation. In a passive system, only the stimulus fiber can supply this energy. Hair bundles are active, however, for they can sustain spontaneous oscillations. As a consequence, both the stimulus and the hair bundle's activity can in principle power motion.

To estimate the hair bundle's active contribution to its motion, we calculated the average amount of energy dissipated per cycle of stimulation, $\overline{W}_D$, and compared it to the average work done by the stimulus fiber, $\overline{W}_{SF}$. An estimate of the average work per cycle provided by the hair cell's active process, $\overline{W}_A$, followed from a condition of energy balance,

$$\overline{W}_D + \overline{W}_{SF} + \overline{W}_A = 0. \qquad [1]$$

Note that, because work done against the linear elasticity of the hair bundle is recovered, there is no average elastic work over a cycle. If $\overline{W}_A > 0$, then the hair cell provided useful work and amplified its input.

The responses to stimulation of 12 spontaneously active hair bundles were analyzed in detail for fiber-base displacements of ±5 nm to ±30 nm and frequencies of 5–23 Hz. Every bundle

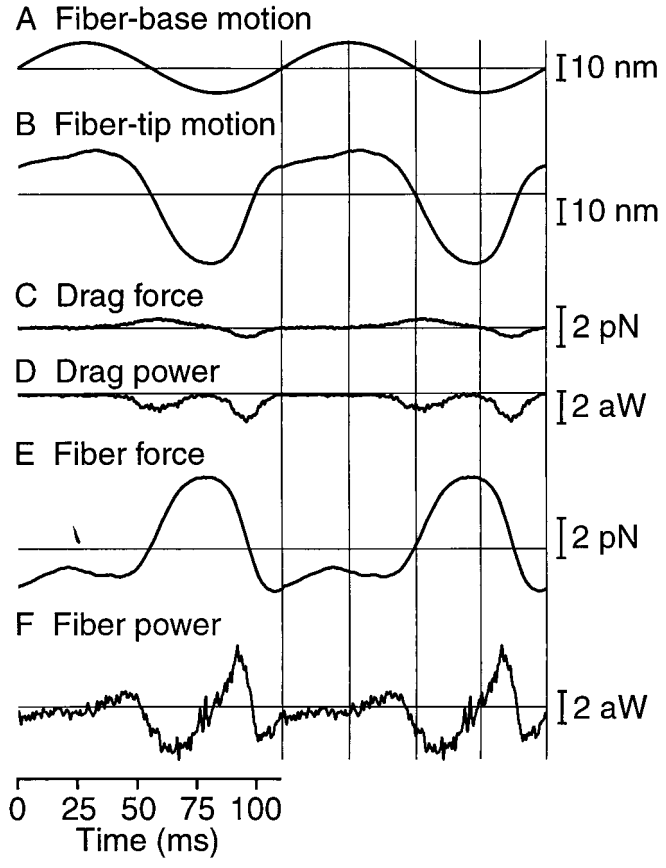

Fig. 2. Analysis of a typical response to mechanical stimulation of an active hair bundle. (*A*) The fiber's base motion, $X_B(t)$, reflected ±10-nm sinusoidal stimulation at 9 Hz, a frequency below the cell's characteristic frequency of 14 Hz. (*B*) The fiber's tip motion, $X(t)$, was more than double the magnitude of stimulation and exhibited a phase lead. (*C*) The viscous drag force, $F_D(t)$, continuously opposed hair-bundle motion. (*D*) Because viscous dissipation continuously withdrew energy from the hair bundle, the instantaneous viscous-drag power, $P_D(t)$, was negative. (*E*) The elastic force exerted by the stimulus fiber on the hair bundle, $F_{SF}(t)$, was dominated by the bundle's elastic reactance. (*F*) The power provided by the stimulus fiber, $P_{SF}(t)$, was greatest during the fast components of the fiber's tip motion. The fiber resisted negatively directed hair-bundle movement but powered motion in the opposite direction. Each record, the average of 21 cycles of oscillation, has been duplicated to emphasize its periodic features; the vertical lines facilitate comparison of response phases.

displayed amplification, which was most apparent at small stimulus amplitudes (Fig. 2*A*). The responses retained the main characteristics of spontaneous oscillations, for they deviated significantly from sine waves: in each cycle, large, fast strokes were followed by slower hair-bundle movements of comparatively small size. The energy dissipation could be deduced from the motion of the fiber's tip, $X(t)$ (Fig. 2*B*). The drag force acting on a hair bundle and the attached stimulus fiber, $F_D(t)$, was proportional to the bundle's velocity:

$$F_D = -(\xi_{HB} + \xi_{SF})\frac{dX}{dt}, \qquad [2]$$

in which ξ_{HB} and ξ_{SF} are the drag coefficients of respectively the bundle and the fiber. Although we measured the drag coefficient of each fiber, we approximated that of each hair bundle as 127 $nN{\cdot}s{\cdot}m^{-1}$, the average value from a previous study (23). The drag power, $P_D(t)$, or amount of energy dissipated by viscosity per unit time, then was

$$P_D = F_D \cdot \frac{dX}{dt} \approx -(\xi_{HB} + \xi_{SF})\left(\frac{\Delta X}{\Delta t}\right)^2. \qquad [3]$$

Here ΔX is the measured increment between successive hair-bundle positions and Δt is the time interval separating them. Note that $P_D(t)$ was always negative. Viscous dissipation was dominant during fast movements of the bundle and fiber (Fig. 2 *C* and *D*). By integrating the drag power over a cycle, we calculated $\overline{W}_D$. $\overline{W}_D$ also could be obtained from the area enclosed by the curve $F_D(X)$:

$$\overline{W}_D = \oint F_D \cdot dX. \qquad [4]$$

In the present instance, $\overline{W}_D = -39$ zJ (Fig. 3*A*).

The average work performed by the stimulus fiber, $\overline{W}_{SF}$, was similarly given by

$$\overline{W}_{SF} = \oint F_{SF} \cdot dX = \oint P_{SF} \cdot dt, \qquad [5]$$

in which the force supplied by the fiber, F_{SF}, stemmed from the Hooke's Law relation

$$F_{SF} = K_{SF}(X_B - X). \qquad [6]$$

Here $X_B(t)$ is the motion of the fiber's base (Fig. 2*A*) and K_{SF} is the fiber's calibrated stiffness. The power delivered by the fiber, P_{SF}, was

$$P_{SF} = F_{SF} \cdot \frac{dX}{dt} \approx K_{SF}(X_B - X)\frac{\Delta X}{\Delta t}. \qquad [7]$$

Note that the stimulus fiber powered the bundle during positively directed bundle movement, for it provided positive work as measured as the area under the curve $P_{SF}(t)$. In contrast, the fiber resisted hair-bundle motion during negative motion, for it withdrew energy from the bundle (Fig. 2 *E* and *F*). Interestingly, the bundle's motion was asymmetrical: the upstroke was faster than the downstroke. As a result, the net work, $\overline{W}_{SF}$, was negative (Fig. 3*A*): $\overline{W}_{SF} = -40$ zJ. This result could not occur in a passive system.

The hallmark of amplification is power gain, the amplifier's contribution of energy to the response. In the present example, the total external work, the sum of the viscous energy dissipation and the fiber's work, was negative: $\overline{W}_D + \overline{W}_{SF} = -79$ zJ. During each cycle of stimulation, the hair cell therefore must have provided the work $\overline{W}_A = +79$ zJ ($\sim 20\ kT$) to amplify the mechanical response and thus to sustain hair-bundle motion.

The sign of the work provided by the stimulus fiber was determined by the relation between the frequency of stimulation and the cell's characteristic frequency. When a hair bundle was driven slower than this frequency, stimulation slowed bundle motion and $\overline{W}_{SF}$ was consequently negative (Fig. 3*A*). Note that in this case the movement of the fiber's tip led that of the base, so that the hair bundle constantly provided work. In contrast, when a bundle was moved faster than its characteristic frequency, the fiber worked to speed the bundle; in this instance, the fiber's tip motion lagged that of its base. Even though $\overline{W}_{SF}$ was positive, this value did not preclude power gain: $\overline{W}_A$ remained positive so long as $\overline{W}_{SF}$ was sufficiently small (Fig. 3*B*). When operating at the cell's characteristic frequency, the fiber performed no net work and $\overline{W}_A = -\overline{W}_D > 0$.

As a bundle fatigued after prolonged stimulation, its properties came to resemble those of a passive system. Even when the hair bundle was driven below its characteristic frequency, the work done by the fiber was positive in sign and comparable in

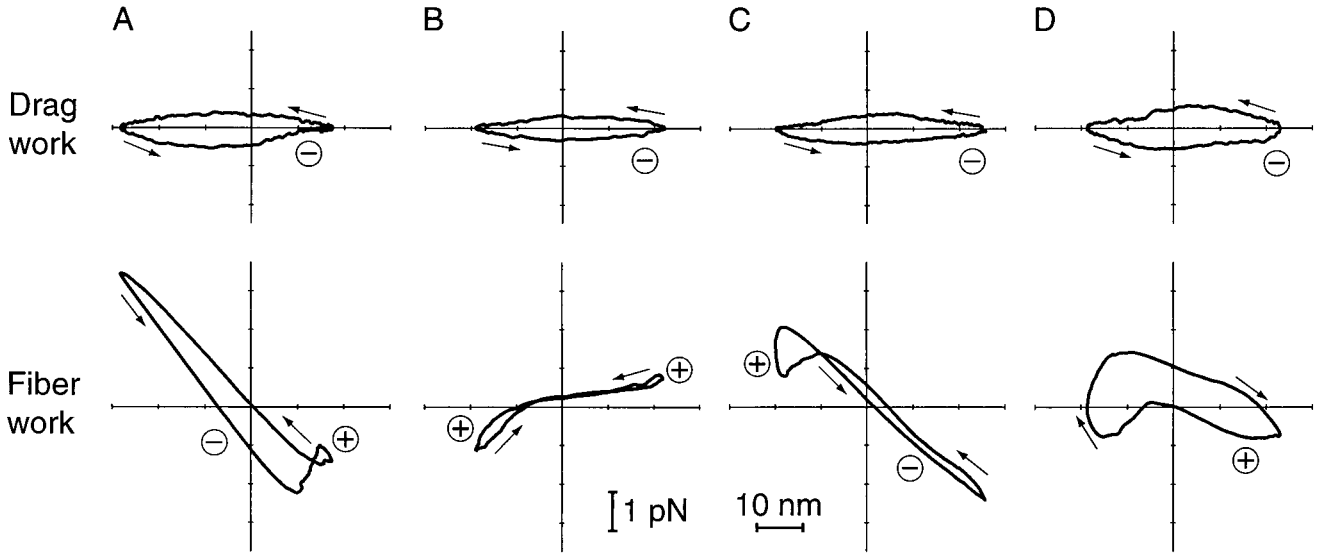

Fig. 3. The force exerted on the hair bundle by viscous drag, F_D (*Upper*), or by the stimulus fiber, F_{SF} (*Lower*), versus the fiber's tip motion, X. Because the hair bundle's movement was periodic, these graphs are closed. The areas enclosed by the curves give respectively the average energy dissipated by viscous drag, $\overline{W}_D$, and the average work provided by the stimulus fiber, $\overline{W}_{SF}$, during one period. The arrows indicate the direction of circulation around a cycle: clockwise circulation signals positive work that powered the hair bundle, whereas motion in the opposite direction reflects negative work that withdrew energy from the bundle. (*A*) The hair bundle analyzed in Fig. 2 was deflected with a ±10-nm stimulus at a frequency of 9 Hz, lower than the hair bundle's characteristic frequency of 14 Hz. Here $\overline{W}_D = -39$ zJ, $\overline{W}_{SF} = -40$ zJ, and thus $\overline{W}_A = +79$ zJ. (*B*) Another hair bundle was driven with a ±30-nm deflection at a frequency of 8 Hz, near the characteristic frequency of 8.5 Hz. In this instance $\overline{W}_D = -37$ zJ, $\overline{W}_{SF} = +3$ zJ, and therefore $\overline{W}_A = +34$ zJ. (*C*) A third bundle received a ±13-nm deflection at 7 Hz, a frequency just below its characteristic frequency of 8 Hz. Here $\overline{W}_D = -42$ zJ, $\overline{W}_{SF} = -6$ zJ, and thus $\overline{W}_A = +48$ zJ. (*D*) After the same cell had fatigued during protracted stimulation, a record was obtained with ±18-nm stimulation at 13 Hz, a frequency lower than the characteristic frequency of 16 Hz. As a consequence of the declining active process, $\overline{W}_D = -49$ zJ, $\overline{W}_{SF} = +50$ zJ, and consequently $\overline{W}_A = -1$ zJ.

magnitude to the energy dissipated against vicosity (Fig. 3 *C* and *D*).

Discussion

The three recognized manifestations of the inner ear's active process are mechanical amplification, nonlinear responsiveness, and otoacoustical emission. Correlates of all three phenomena now have been observed in hair cells of the frog's sacculus. As shown here and previously (13, 15), the hair bundles of this receptor organ can oscillate spontaneously, a potential basis for spontaneous otoacoustic emission. The bundles can produce mechanical distortion products (24), the root of synchronously evoked otoacoustic emission. The present observations demonstrate that saccular hair bundles also can amplify mechanical inputs. Active hair-bundle motion therefore appears likely to constitute the amplificatory process in this receptor organ.

Hair bundles *in vivo* are in most instances attached to an accessory structure such as a tectorial or otolithic membrane. Unlike the bundles in our experiments, in which these structures had been removed, hair bundles in an intact organ are elastically coupled through the accessory structure so that their movements should be synchronized. Despite occasional failures by individual hair bundles, the amplification of small mechanical stimuli by an ensemble of hair cells that operate in conjunction is likely to be both more forceful and more consistent than that observed here.

Whether spontaneous oscillations persist when the hair bundles are attached to the otolithic membrane remains uncertain. Because the transduction of spontaneous hair-bundle movements would send meaningless signals to the brain, unstimulated hair cells might take advantage of a quiescent active process. Small stimuli would, however, trigger the active process. Consistent with this idea, one model of the amplificatory process (20) predicts the existence of a Hopf bifurcation: only when a control parameter reaches a critical value do the hair cells produce spontaneous oscillations. Because the bifurcation corresponds to an infinite gain, hair cells are likely to be poised nearby to maximize tuning and amplification.

Our determination of the active work done by the hair bundle doubtlessly represents a lower estimate. First, because up to 40 cycles were averaged in the analysis of each record, the actual viscous dissipation exceeded that presented here. When experimental records are inspected on a cycle-by-cycle basis, slight phase differences are apparent in the rapid components of hair-bundle movement. As a consequence, the rapid components of bundle motion were in general faster than those in the average record. Second, it is conceivable that the hair bundle experiences energy dissipation in addition to that contributed by viscosity. One potential source of additional dissipation is entropic in nature (5, 25). As the ensemble of transduction channels in a stimulated hair bundle progresses from entirely closed toward the open state, or from the open toward the closed state, the entropy of the system increases. If the transition occurs so quickly that the transduction channels are out of thermal equilibrium, unrecoverable mechanical work must be used to effect the transition. If the bundle overcomes such additional sources of dissipation to achieve the performance reported here, its energy production must be still greater than we appreciate.

This study raises two important issues. The first concerns the power source of active hair-bundle motion. The candidates to power movement include the myosin molecules that mediate adaptation (reviewed in refs. 18 and 19) and the channels involved in mechanoelectrical transduction (14, 15, 20). It remains conceivable, though, that the bundle simply serves as a lever to deliver power generated elsewhere in the hair cell. The second issue concerns the phases of a cycle of oscillation during which the active process does useful work. For the bundle whose response is depicted in detail, the prominent pulse of negative power associated with the stimulus fiber (Fig. 2*F*) suggests that the bundle delivered power during the negatively directed phase of bundle movement. Work done during this phase may reflect

channel reclosure promoted by Ca^{2+} entry through transduction channels (14, 20). The bundle apparently did work as well during the positively directed phase of movement, a period when elastic energy stored in deflected stereocilia (reviewed in ref. 26) was released.

The capacity to amplify mechanical stimuli was associated with spontaneous movements of hair bundles. This oscillation resumed after perturbation by a stimulus (Fig. 1 *A* and *E*), so it represented a limit cycle. Because the time constant of the movement's slow phase, ~30 ms, resembled that of mechano-electrical adaptation (13, 27, 28), the spontaneous motion between extreme bundle positions appeared to be set by the adaptation motor.

The active responses observed in this study were largely tuned to relatively low frequencies for the bullfrog's sacculus, in which the best excitatory frequencies of afferent nerve fibers lie in the range 5 to 130 Hz (29). Three factors may have contributed to the observation of low response frequencies. First, the protease treatment required to free hair bundles from the otolithic membrane may have damaged the amplificatory apparatus and slowed its action. Such proteolytic treatments are known to affect numerous proteins in the stereociliary membrane (30). Next, it is possible that the Ca^{2+} concentration used was lower than that to which the apical surfaces of hair cells are exposed *in vivo*. Because the frequency of spontaneous hair-bundle oscillation rises (data not shown) and bundle twitches become faster (15, 31) as the Ca^{2+} concentration increases, the active process is clearly Ca^{2+}-dependent. Finally, and perhaps most importantly, we concentrated our measurements on hair bundles whose spontaneous oscillations were readily apparent by eye. Several randomly selected bundles were tuned to higher frequencies than those chosen on the basis of visible movement.

Hair bundles exhibited both spontaneous oscillations and mechanical amplification in a medium with a drastically reduced K^+ concentration and thus a greatly diminished transduction current. This finding supports the inference that Ca^{2+}, which was present at roughly its physiological concentration, is key in the hair bundle's active process. Note that perfusion of the scala media with a solution similar to NMDG endolymph may provide a means of discriminating between the two candidates to underlie the active process of the mammalian cochlea. In the absence of a normal K^+ current, active bundle motility would be expected to continue, whereas electromotility would be eliminated. Measurements of basilar-membrane vibration then might reveal which process mediates cochlear amplification.

The presence of amplification in the frog's sacculus suggests that the hair cell's active process is more widespread than the name "cochlear amplifier" implies. Hair-bundle amplification should prove useful not only in the cochlea, but in any receptor organ that must counter damping forces, especially those associated with oscillatory stimuli. The frog's sacculus, for example, is a receptor for ground-borne vibration and low-frequency sound (29, 32). Amplification also might be appropriate for hair cells of the lateral-line organ, in which nonlinear mechanical responses may signal a contribution of hair-bundle motion to an active process (33). Because hair bundles are ubiquitous in the vertebrate inner ear, hair-bundle amplification also remains a candidate to account for other manifestations of the ear's active process, including the mammalian cochlear amplifier.

We thank Drs. A. Libchaber, M. Magnasco, A. Mehta, M. Ospeck, and E. Siggia and Mr. Y. Choe for helpful discussions and Mr. B. Fabella for computer programming. Drs. P. G. Gillespie and E. A. Lumpkin and members of our research group provided critical comments on the manuscript. This research was supported by National Institutes of Health Grant DC00241. P. M. is an Associate and A. J. H. an Investigator of Howard Hughes Medical Institute.

1. Hudspeth, A. J. (1997) *Curr. Opin. Neurobiol.* **7,** 480–486.
2. Gold, T. (1948) *Proc. R. Soc. London Ser. B* **135,** 492–498.
3. Probst, R. (1990) *Adv. Otorhinolaryngol.* **44,** 1–91.
4. Ruggero, M. A. (1992) *Curr. Opin. Neurobiol.* **2,** 449–456.
5. Markin, V. S. & Hudspeth, A. J. (1995) *Annu. Rev. Biophys. Biomol. Struct.* **24,** 59–83.
6. Dallos, P. (1992) *J. Neurosci.* **12,** 4575–4585.
7. Nobili, R., Mammano, F. & Ashmore, J. (1998) *Trends Neurosci.* **21,** 159–167.
8. Hudspeth, A. J. (1989) *Nature (London)* **341,** 397–404.
9. Preyer, S., Renz, S., Hemmert, W., Zenner, H.-P. & Gummer, A. W. (1996) *Aud. Neurosci.* **2,** 145–157.
10. Manley, G. A. & Köppl, C. (1998) *Curr. Opin. Neurobiol.* **8,** 468–474.
11. Yates, G. K. & Kirk, D. L. (1998) *J. Neurosci.* **18,** 1996–2003.
12. Crawford, A. C. & Fettiplace, R. (1985) *J. Physiol.* **364,** 359–379.
13. Howard, J. & Hudspeth, A. J. (1987) *Proc. Natl. Acad. Sci. USA* **84,** 3064–3068.
14. Howard, J. & Hudspeth, A. J. (1988) *Neuron* **1,** 189–199.
15. Benser, M. E., Marquis, R. E. & Hudspeth, A. J. (1996) *J. Neurosci.* **16,** 5629–5643.
16. Marquis, R. E. & Hudspeth, A. J. (1997) *Proc. Natl. Acad. Sci. USA* **94,** 11923–11928.
17. Denk, W. & Webb, W. W. (1992) *Hear. Res.* **60,** 89–102.
18. Hudspeth, A. J. & Gillespie, P. G. (1994) *Neuron* **12,** 1–9.
19. Gillespie, P. G. & Corey, D. P. (1997) *Neuron* **19,** 955–958.
20. Choe, Y., Magnasco, M. O. & Hudspeth, A. J. (1998) *Proc. Natl. Acad. Sci. USA* **95,** 15321–15326.
21. Denk, W., Keolian, R. M. & Webb, W. W. (1992) *J. Neurophysiol.* **68,** 927–932.
22. Lumpkin, E. A., Marquis, R. E. & Hudspeth, A. J. (1997) *Proc. Natl. Acad. Sci. USA* **94,** 10997–11002.
23. Denk, W., Webb, W. W. & Hudspeth, A. J. (1989) *Proc. Natl. Acad. Sci. USA* **86,** 5371–5375.
24. Jaramillo, F., Markin, V. S. & Hudspeth, A. J. (1993) *Nature (London)* **364,** 527–529.
25. Hudspeth, A. J., Roberts, W. M. & Howard, J. (1989) in *Cochlear Mechanisms: Structure, Function and Models*, eds. Wilson, J. P. & Kemp, D. T. (Plenum, New York), pp. 117–123.
26. Hudspeth, A. J. (1992) in *Sensory Transduction*, eds. Corey, D. P. & Roper, S. D. (Rockefeller Univ. Press, New York), pp. 357–370.
27. Eatock, R. A., Corey, D. P. & Hudspeth, A. J. (1987) *J. Neurosci.* **7,** 2821–2836.
28. Hacohen, N., Assad, J. A., Smith, W. J. & Corey, D. P. (1989) *J. Neurosci.* **9,** 3988–3997.
29. Yu, X., Lewis, E. R. & Feld, D. (1991) *J. Comp. Physiol. A* **169,** 241–248.
30. Gillespie, P. G. & Hudspeth, A. J. (1991) *J. Cell Biol.* **112,** 625–640.
31. Jaramillo, F., Howard, J. & Hudspeth, A. J. (1990) in *The Mechanics and Biophysics of Hearing*, eds. Dallos, P., Geisler, C. D., Matthews, J. W., Ruggero, M. A. & Steele, C. R. (Springer, Berlin), pp. 26–33.
32. Koyama, H., Lewis, E. R., Leverenz, E. L. & Baird, R. A. (1982) *Brain Res.* **250,** 168–172.
33. van Netten, S. M. & Khanna, S. M. (1994) *Proc. Natl. Acad. Sci. USA* **91,** 1549–1553.